

## Barley Straw Ash: Pozzolanic Activity and Comparison with other Natural and Artificial Pozzolans from México

Carlos Cobreros,<sup>a,\*</sup> José Luis Reyes-Araiza,<sup>a</sup> Alejandro Manzano-Ramírez,<sup>b</sup> Rufino Nava,<sup>a</sup> Mario Rodríguez,<sup>c</sup> Mauricio Mondragón-Figueroa,<sup>b</sup> Luis Miguel Apátiga,<sup>c</sup> and Eric M. Rivera-Muñoz<sup>c</sup>

The construction industry is one of the largest and most active growth sectors worldwide. It presents an important environmental impact, and one way to reduce the impact of the construction activity is to substitute pozzolanic materials for ordinary Portland cement. In this work, barley straw, barley straw ash, and other natural and artificial pozzolans from Mexico were characterized and compared. Also, the pozzolanic activity of barley straw ash was compared with the pozzolanic properties of some natural and artificial pozzolans from Mexico. Materials considered included recycled dust of fired clay brick, fly ash, volcanic ash, and wheat straw ash.

*Keywords:* Straw Ash; Pozzolana; Sustainable construction; Fired clay brick

*Contact information:* a: Facultad de Ingeniería, División de Investigación y Posgrado, Universidad Autónoma de Querétaro, Av. Cerro de las Campanas s/n. Colonia Las Campanas, C.P. 76010, Santiago de Querétaro, Qro., México; b: CINVESTAV-Querétaro. Libramiento Norponiente # 2000, C. P. 76230, Fraccionamiento Real de Juriquilla. Querétaro, Qro. México; c: Departamento de Nanotecnología, Centro de Física Aplicada y Tecnología Avanzada, Universidad Nacional Autónoma de México-Campus Juriquilla. Boulevard Juriquilla 3001, C. P. 76230, Querétaro, Qro. México;

\* Corresponding author: carlos\_cobreros@yahoo.es

### INTRODUCTION

The construction industry is one of the largest and most active growth sectors worldwide. By direct or indirect actions, it consumes over 50% of the global energy (Edwards 2008), is responsible for 30% of CO<sub>2</sub> emissions, and consumes more raw material than any other industrial activity (about 3,000 Mt/year, almost 50% of overall consumption) (Pacheco-Torgal and Jalali 2012). It is primarily based on the use of Portland cement and concrete. The manufacture of cement and concrete based on Portland cement for construction contributes about 5% of the anthropogenic CO<sub>2</sub> emissions to the atmosphere (Worrel *et al.* 2001; Gartner and MacPhee 2011). One way to reduce the impact of the construction activity is to substitute pozzolanic materials for ordinary Portland cement.

Different international standards define pozzolans as "silico-aluminous or siliceous materials which themselves have little or no cementitious or hydraulic activity, but finely divided and in the presence of water can react with calcium hydroxide (Ca(OH)<sub>2</sub>) at environmental temperature to form compounds having cementitious properties" (ASTM C-125-13b (2013)).

Pozzolans can be obtained from both natural and industrial sources. Natural pozzolans, which do not require transformation processes to be activated (Villar Cociña *et al.* 2011), include silica-alumina materials such as volcanic ash, silica fume, and diatomaceous earth, and minerals such as pumice, opal, and slate. Natural calcined and

artificial pozzolans, which need chemical and mineralogical changes to exhibit their pozzolanic activity, can be obtained from sources such as blast furnace slag, industrial waste generated in the production of iron, the ash of organic materials, and agricultural waste. Recently, studies have shown that artificial and natural pozzolans can have good pozzolanic characteristics (Lima Souza and Dal Molin 2005; Mathur 2005; Martinez-Ramirez *et al.* 2006; Sinthaworn and Nimityongskul 2009; Karade 2010; Amigó *et al.* 2011; Rosell-Lam *et al.* 2011; Villar Cociña *et al.* 2011).

Pozzolans have been studied as a partial substitute for ordinary Portland cement and as cementitious material in combination with lime, providing many benefits (Mathur 2005; Karade 2010): impermeability, durability, resistance to attack by sulfates, workability, and, at older ages, increased mechanical strength, and decreased water absorption and retraction. In addition, with the use of pozzolans instead of Portland cement, the alkali-aggregate reaction is reduced and an economic benefit, by reducing the Portland cement consumption, is obtained without the loss of mechanical properties (Biricik *et al.* 1999; Lanas and Pérez Bernal 2004).

The application of agricultural waste in the production of pozzolanic material can also be considered technically feasible and has been the focus of recent studies (Akhras and Abu-Alfoul 2002). Accumulation of unmanaged agricultural waste, especially in developing countries, has increased environmental concern. Using agricultural waste instead of conventional materials offers a substantial environmental contribution (Lima *et al.* 2012), helping to solve the problems of pollution and conservation of natural resources for future generations (Madurwar *et al.* 2013). With the calcination of organic materials, thermal decomposition occurs and ash is produced in a fine particle size; when mixed with lime, this can produce a material with binding properties (Biricik *et al.* 1999). The silica content and the activation conditions (temperature and retention time in an oven) are important for determining the pozzolanic activity (Khangaonkar *et al.* 1992; Payá *et al.* 2001; Sánchez de Rojas *et al.* 1999; Payá *et al.* 2001; Frías *et al.* 2007).

There have been several studies of the pozzolanic properties of bagasse ash (Rukzon and Chindaprasirt 2012; Madurwar *et al.* 2013), rice husk ash (Ramasamy and Biswas 2008; Rukson and Chindaprasirt 2014), and bamboo leaf ash (Villar Cociña *et al.* 2008, 2011).

Biricik *et al.* (1999) studied the production of pozzolanic material from wheat straw ash (WSA), tested with calcination at different temperatures and times, to determine the content of SiO<sub>2</sub> and ash. Biricik *et al.* (1999), Bensted and Munn (2000), and Al-Akhras and Abu-Alfoul (2002) later, with a study of the contribution of the WSA in autoclaved mortars, confirmed that the ash obtained from wheat straw, well burnt and finely ground, could be used as a pozzolanic material. They also concluded that the quality of the material depends on the time, calcination temperature, cooling time, and milling conditions. It was also determined that the wheat straw had 8.6% ash, with a silica content of 73% in the ash. The straw burned at 570 and 670 °C had pozzolanic properties, and the first one had higher pozzolanic property than the straw burned at 670 °C; however, there have not been many studies about other kinds of cereal straw ash, such as barley straw ash or oat straw ash, even though they are important crops around the world.

To characterize the pozzolans, the literature refers to studies of crystalline phases and mineralogic composition analysis by X-ray diffraction (XRD) (Marín *et al.* 2011), morphology and structure/microstructure by scanning electron microscope (SEM) (Villar-Cociña *et al.* 2011; Cristelo *et al.* 2012), energy dispersive spectroscopy (EDS)

microanalyses to determine the chemical composition (Cristelo *et al.* 2012), chemical composition by X-ray fluorescence (XRF) (Marín *et al.* 2011), maximum grain size, and fineness modulus (Lima *et al.* 2012).

There are different methods, such as chemical, physical, and mechanical, which are classified as direct and indirect (Malhorta and Dave 1999), to determine whether a material such as agricultural waste or pozzolana is a pozzolanic material, but the common parameter to determine this is dependent on the reactive silicon and alumina content and the percentage of amorphous structural phase. Other common parameters are maximum grain size, fineness modulus, and the measure of the reaction between the pozzolana and  $\text{Ca}(\text{OH})_2$ , where the reactivity and activity of the pozzolana can be determined (Larbi and Bijen 1990; Taylor 1997; Malhotra and Dave 1999). Other works have studied compressive strength with different combinations of Portland cement or lime (Cristelo *et al.* 2012; Lima *et al.* 2012).

Recent studies to evaluate pozzolana activity have focused on the kinetic coefficients of this reaction as an acceptable and rigorous criterion for evaluating the pozzolanic activity of the materials (Sanchez de Rojas *et al.* 1999; Mostafa *et al.* 2001; Poon *et al.* 2001; Villar Cociña *et al.* 2008, 2011) because of the nature of the materials and the complex mechanisms of the interaction between pozzolana and  $\text{Ca}(\text{OH})_2$ . However, it is difficult to determine the mechanism and kinetics of the pozzolanic reaction accurately, because of their complexity mentioned earlier. For this reason, it is interesting to perform a profound study of the pozzolanic reaction kinetics. Some mathematical models have been developed to describe the pozzolanic reaction kinetics, but these models do not always coincide with the experimental results for all reaction times (Khangaonkar *et al.* 1992; Villar-Cociña *et al.* 2003; Frías *et al.* 2005; Villar Cociña *et al.* 2008, 2011).

In this work, barley straw, barley straw ash, and other natural and artificial pozzolans from Mexico, such as wheat straw ash, volcanic ash, fired clay brick, and fly ash, were characterized. The pozzolanic activity of barley straw ash was compared with the pozzolanic properties of recycled dust of fired clay brick, fly ash, volcanic ash, and wheat straw ash, all being natural and artificial pozzolans from Mexico.

To determine this pozzolanic activity, the water-soluble fraction, fineness, lime-pozzolana compressive strength development, and lime consumption (using a conductometric method) were also evaluated.

In addition, analysis of the evolution of crystalline phases during the pozzolanic reaction was performed using X-ray diffraction (XRD), and the evolution of micro-morphology during the pozzolanic reaction was evaluated using a scanning electron microscope (SEM).

## EXPERIMENTAL

### Materials

The material consisted principally of barley straw ash (BSA) from barley straw of the El Bajío region (Mexico). It was calcined outdoors without control, mimicking the conventional burning methods of farmers in the region. Other materials studied were wheat straw ash (WSA) from wheat straw of the El Bajío region (Mexico), calcined outdoors without any control; recycled dust of fired clay brick (BD), coming from waste bricks from a traditional production plant in the region; fly ash (FA), coming as residue from a

thermoelectric plant in Coahuila (Mexico); and volcanic ash (VA), collected from the last big eruption of ash of the Popocatepetl volcano in Puebla (Mexico), in June 2013. The pozzolanic materials were ground and sieved to 75  $\mu\text{m}$  to obtain particle sizes and fineness similar to that of Portland cement.

## Methods

### *Characterization of barley straw ash and other pozzolanic materials*

Chemical composition was determined using trace element analysis with micro X-ray fluorescence (MXRF). A high-performance micro-spot X-ray source for SEM (Bruker XL 30 ESEM) was also used. This kind of analysis cannot quantify light elements such as carbon, nitrogen, oxygen, fluorine, or sodium. Crystalline phases and mineralogical compounds were determined using XRD. Wide-angle XRD analysis was performed on a Rigaku Ultima IV diffractometer with operating conditions of 40 KV and 30 mA, with a  $\text{CuK}\alpha$  radiation wavelength of  $\lambda = 1.5406 \text{ \AA}$ . Data were collected from 5 to  $80^\circ$  on a  $2\theta$  scale with a solid state D/teX-ULTRA detector with a speed of  $10^\circ/\text{min}$  and a sampling rate of 0.02 sec. Spectrum analysis software, MDI Jade V 5.0.37, was used. BSA morphology and microstructural analysis using a scanning electron microscope (SEM) and quantitative chemical composition micro-analysis using energy dispersive spectroscopy (EDS) were carried out. The micrographs were generated by a computer program. Scanning electron microscopy was performed on a JEOL JSM-6060LV, with a spot size of 45, WD 8, acceleration of 20 V, and a micron-marker of 10  $\mu\text{m}$ .

### *Barley straw ash pozzolanic activity analysis and comparison with other natural and artificial pozzolanas*

To determine the water-soluble fraction (WSF), 10 g of a dried pozzolana sample (dried at a constant weight in an oven at 105 to 110  $^\circ\text{C}$ ) was placed in a 200-mL Erlenmeyer flask. Then, 100 mL of distilled water at 23  $\pm$  2  $^\circ\text{C}$  was added to the flask. It was well shaken by hand until no lumps were observed, which indicated that all of it was dissolved; then, with a mechanical shaker, it was agitated at room temperature for a period of 1 h. The material was placed in a sintered-glass crucible, and all residues were washed from the flask into the crucible with distilled water. The crucible was dried to constant weight in an oven at 105  $^\circ\text{C}$  for 24 h. The weight loss is equal to the weight of dissolved material lost upon evaporation. The percentage of water-soluble fraction was calculated by multiplying the weight loss in grams by 10. The VA was studied only grounded and sieved to 75  $\mu\text{m}$ .

Particle size was determined by sieving 100 g of dried pozzolana in sieves number 4 (4.75 mm), 8 (2.36 mm), 16 (1.18 mm), 30 (600  $\mu\text{m}$ ), 50 (300  $\mu\text{m}$ ), 100 (150  $\mu\text{m}$ ), and 200 (75  $\mu\text{m}$ ). The partial retention and cumulative retention, and particularly the amount retained by sieves number 30 (600  $\mu\text{m}$ ) and 200 (75  $\mu\text{m}$ ), were examined.

Size distribution by intensity (SDI) was studied by analyzing the percentage of particles in relation to the diameter of the particles of dried pozzolana. The pozzolana was sieved by sieve number 200. A total of 0.50 mg of pozzolana was dispersed in distilled water, and the procedure was carried out in a Zetasizer Nano S analyzer at 25  $^\circ\text{C}$  for 60 s with a measurement position of 1.25 mm.

### *Lime-pozzolana reaction (pozzolanic activity)*

To study the pozzolanic activity of these materials, the electrical conductivity measurement method (ECMM) was used. The conductometric method used was based on

the method described by Villar-Cociña *et al.* (2008, 2011). This method follows the conductivity of a pozzolan - calcium hydroxide solution (CHS) with reaction time. A total of 100 mL of saturated  $\text{Ca}(\text{OH})_2$  solution was mixed with 2.10 g of pozzolan and magnetically stirred. The  $\text{Ca}(\text{OH})_2$  was mixed with deionized water and stirred for 2 h to obtain the CHS; after that, the CHS was maintained at rest for 24 h. The pozzolan was mixed with the CHS, after which the conductivity measurements for 28 days (675 h) started. The measurements of conductivity were made with a calibrated PS-2116 PASCO conductivity sensor for aqueous solutions, at  $25 \pm 2$  °C room temperature at different times. The pozzolanic activity is shown by the relationship between the conductivity and the reaction time (h).

#### *Lime-pozzolana compressive strength development*

Lime-pozzolana compressive strength development (adaptation based on ASTM C 593-95 (Reapproved 2000)) testing was carried out in accordance with the applicable portions of ASTM Test Method C 109 and Practice C 305. Strength testing was conducted on three specimens of each age. Batches were of a size sufficient to make six specimens and consisted of proportions of the dry materials as follows: hydrated lime 180 g, pozzolana (dry basis) 360 g, and graded standard sand 1480 g. Mixing water, measured in milliliters, was added to produce a flow of 65 to 75, expressed as weight percent of the combined lime and pozzolana. The lime and pozzolana were blended together in a closed container. Mixing was done by adding the blended lime and pozzolana to the water and allowing it to stand for 1 min. The flow was determined in accordance with ASTM Test Method C 109, with the exception of 10 drops in 6 s instead of the stated 25 drops in 15 s. Immediately after the completion of the flow test, mortar specimens were molded in accordance with Test Method C 109.

When molding was completed, the filled molds were molded in the vapor immediately above water at  $54 \pm 5$  °C in a closed vapor oven with the top surface protected from the drip. The specimens in the molds remained in the vapor for a period of 7 days, after which they were removed from the vapor and cooled to  $23 \pm 5$  °C in a saturated air environment. When the specimens were cool, they were removed from the molds and stored at  $23 \pm 5$  °C at 95 to 100% relative humidity until the time of the compressive strength test of 21 days was reached.

#### *The evolution of crystalline phases and morphology during the pozzolanic reaction*

The evolution of crystalline phases during the pozzolanic reaction, analyzed on pozzolana-lime-sand-water specimens after 7 days and 28 days under controlled curing conditions, was studied using X-ray diffraction (XRD) to detect the appearance of new crystalline phases and the disappearance of some phases present in the original pozzolans. The specimens were the same specimens prepared for the lime-pozzolana strength development.

The evolution of morphology and microstructure during the pozzolanic reaction between pozzolana-lime-sand-water specimens after 7 days and 28 days under controlled curing conditions was also studied using the specimens prepared for the lime-pozzolana strength development test. An observation of the specimens by SEM showed the appearance and formation of new microstructures.

## RESULTS AND DISCUSSION

### Characterization of Barley Straw Ash and Other Pozzolanic Materials

The chemical composition of the BSA showed high contents of silica and potassium, 21.15% and 38.03%, respectively, by weight, followed by calcium, sodium, and iron, with percentages of about 10.02%, 4.12%, and 3.50%, respectively (Table 2). The other pozzolans showed high contents of silica and aluminum: 61.32% and 15.64%, respectively, in BD, 53.04% and 21.03%, respectively, in FA, and 50.73% and 14.11%, respectively, in VA. These contents were less in WSA. The BD and FA also had a high content of iron. Further details are shown in Table 1.

**Table 1.** Chemical Composition by Trace Element Analysis with Micro X-Ray Fluorescence (XRF)

	Na (%)	Al (%)	Si (%)	S (%)	K (%)	Ca (%)	Fe (%)
BD	1.56	15.64	61.32	0.39	5.14	4.38	9.18
FA	0.00	21.03	53.04	0.45	3.37	8.51	11.02
VA	4.09	14.11	50.73	0.09	4.49	11.49	11.41
BSA	4.12	2.72	21.15	2.47	38.03	10.02	3.50
WSA	0.41	1.02	31.82	1.50	43.41	9.53	2.37

Figure 1 shows the XRD patterns for BSA. Quartz ( $\text{SiO}_2$ ), sylvite (potassium chloride,  $\text{KCl}$ ), and calcite ( $\text{CaCO}_3$ ) were the primary crystalline compounds detected in the BSA. The PDXL2 V 2.1.3.4 software and the results showed that there was 50% crystallinity in this sample. Also, BSA was compared with the other pozzolans (Fig. 2), where the BD sample showed a higher amorphous phase content, as shown by reduced peaks.

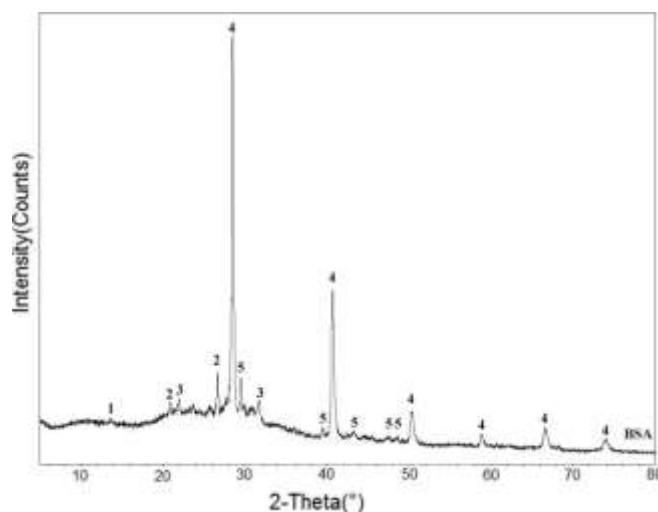


**Fig. 1.** Crystalline phases and compounds by X-ray diffraction (XRD) of BSA: (1) anorthoclase ( $\text{AlSi}_3\text{O}_8$ ), (2) quartz ( $\text{SiO}_2$ ), (3) albite ( $\text{AlSi}_3\text{O}_8$ ), (4) sylvite ( $\text{KCl}$ ), and (5) calcite ( $\text{CaCO}_3$ )

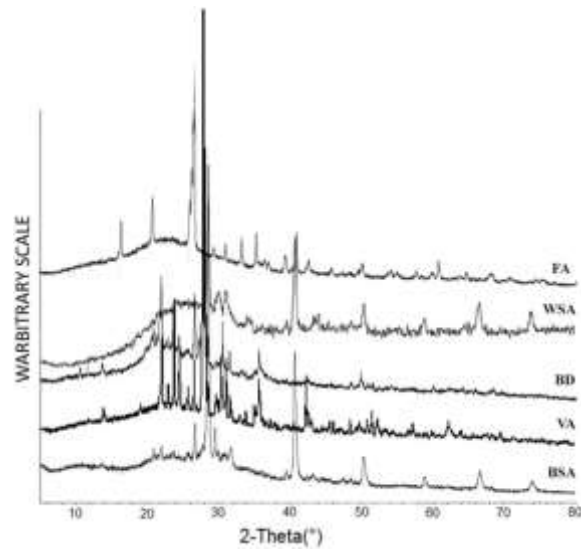


**Fig. 2.** Crystalline phases comparison by X-ray diffraction (XRD) of FA, VA, WSA, BSA, and BD

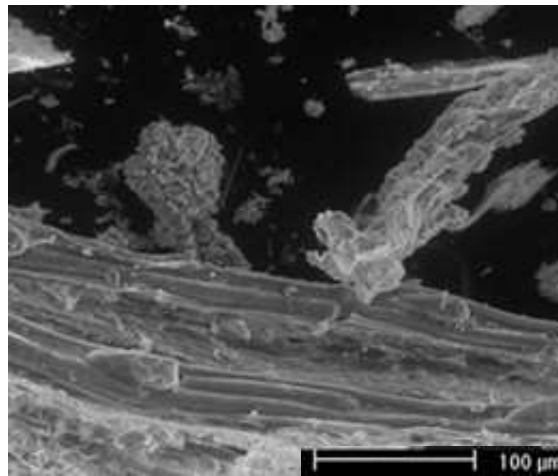


**Fig. 3.** SEM micrograph of BSA at 250x

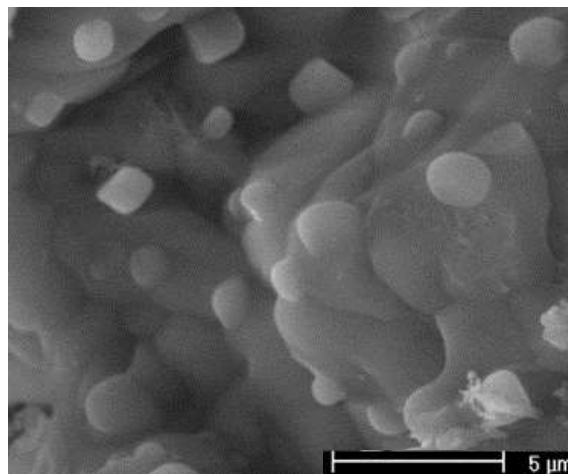


**Fig. 4.** SEM micrograph of BSA at 5000x

The characteristic morphology and microstructure of the BSA, at a magnification of 250x, are shown in Fig. 3. Figure 4 shows some different morphologies, quasi-spheres, as the most characteristic geometry of BSA microstructure.

### Water-Soluble Fraction (WSF)

BSA presented a 33.10 % WSF, more than any other sample, followed by BD and FA, with 31.10 % and 31.20 %, respectively (Table 2). It is important to ensure that there is enough water-soluble fraction to guarantee the reaction between pozzolana and  $\text{Ca}(\text{OH})_2$ ; thus, BSA, BD, and FA showed favorable results.

**Table 2.** Water-Soluble Fraction (WSF) of Pozzolans

	BD	FA	VA	BSA	WSA
WSF(%)	31.10	31.20	5.10	33.10	28.50

### Particle Size (PS)

The study of particle size (PS) by the retention by sieve numbers 30 and 200 showed that BSA had a high percentage of particles above 75  $\mu\text{m}$ , and also some above 600  $\mu\text{m}$ . The best distribution of particles, or the pozzolans with the most fine particles, was found in BD and FA (Table 3).

**Table 3.** Particle Size (PS), by Retention and Cumulative Retention by Sieve Numbers 30 and 200

	Retention 30(600 $\mu\text{m}$ ) (%)	Cumulative Retention 30(600 $\mu\text{m}$ ) (%)	Retention 200(75 $\mu\text{m}$ ) (%)	Cumulative Retention 200(75 $\mu\text{m}$ ) (%)
BD	0.40	0.40	35.93	70.85
FA	0.29	0.29	30.68	49.77
VA	0.62	0.67	2.68	98.95
BSA	2.21	2.21	7.58	94.62
WSA	22.43	22.43	5.12	95.70

### Size Distribution by Intensity (SDI)

As shown in Fig. 6, a significant percentage of fine particles of BSA and a narrow

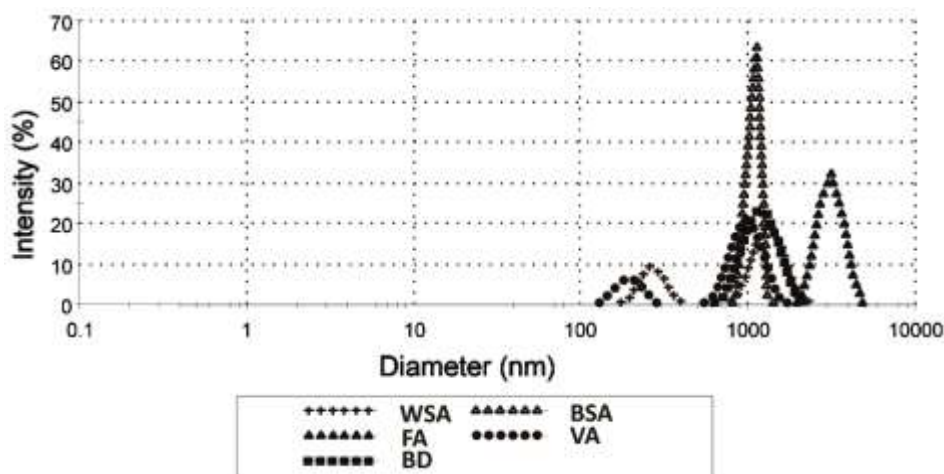


**Fig. 6.** Size distribution by intensity



size distribution by intensity existed in comparison with the other studied pozzolans (Fig. 8). FA presented the worst result, where as WSA and VA had a bimodal distribution of particle size (Fig. 6).

### Lime-Pozzolana Reaction by Electrical Conductivity Measurement Method (ECMM)

The results obtained for the lime-pozzolana reaction by ECMM are shown in Fig. 7, which displays the conductivity ( $\mu\text{S}/\text{cm}$ ) versus reaction time (h). The initial point of each curve was adjusted to have the same starting point to enable comparison. A decrease in the electrical conductivity of the pozzolana/CH system was apparent. This behavior is attributed to the pozzolanic reaction between amorphous silica (Si) and CH to give the formation of gels (C-Si-H), with a corresponding decrease in the CH concentration in the solution (Villar-Cociña *et al.* 2011). A decrease in conductivity in the early stages was observed in all cases. The stabilization of the curve was reached after long periods of time in general, when the reaction was close to completion. The curves for FA and BD decreased faster than the others, which shows a better reaction between the pozzolan and the CH at the early stages. These results are consistent with the results obtained in the lime-pozzolana compressive strength development test.

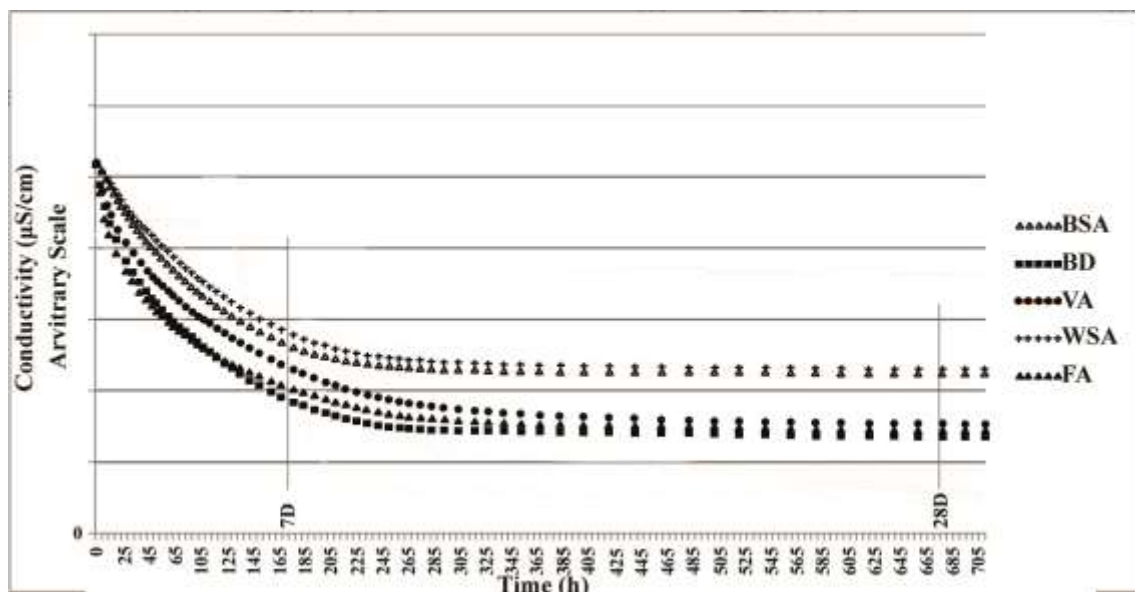
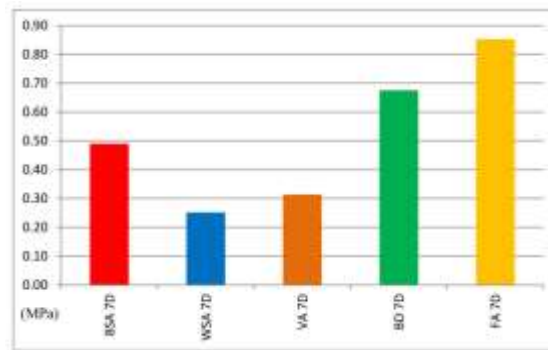


Fig. 7. Lime-pozzolana reaction by electrical conductivity measurement method (ECMM)

### Lime-Pozzolana Compressive Strength Development

Figures 8 and 9 show a comparison of the lime-pozzolana compressive strength development test after 7 days and 28 days, respectively, of curing under controlled conditions. Figure 8 shows that specimens with BSA, compared to the other studied specimens, did not have a bad result after 7 days. At 28 days of curing, no increase in compressive strength was observed for specimens with BSA (Fig. 9). In the first period, specimens with FA had the best development of the compressive strength under the controlled humidity conditions, compared to the other studied specimens (Fig. 8). After 28 days, the best results were for specimens with BD (Fig. 9).



**Fig. 8.** Lime-pozzolana strength development after 7 days in controlled conditions

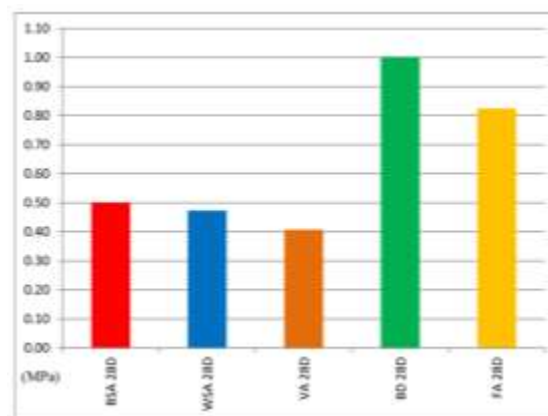


**Fig. 9.** Lime-pozzolana strength development after 28 days in controlled conditions

The evolution of crystalline phases during the pozzolanic reaction was observed using XRD. As the most characteristic samples, BSA, BD, and FA were selected for the comparison. The presence of crystalline phases in the BSA, BD, and FA and the mix of BSA-CH-sand-water, BD-CH-sand-water, and FA-CH-sand-water after 7 days and 28 days was compared (Figs. 10, 11, and 12). The presence of sylvite (KCl), quartz ( $\text{SiO}_2$ ), anorthoclase ( $\text{AlSi}_3\text{O}_8$ ), albite ( $\text{AlSi}_3\text{O}_8$ ), and calcite ( $\text{CaCO}_3$ ) crystalline structures were detected in the original sample of BSA and in the mix of BSA-CH-sand-water after 7 days and 28 days (Fig. 10); on the contrary, sylvite almost disappeared at the 28-day sample or was not clearly detected, while the calcite presence increased. At 7 days, quartz and calcite were the principal crystalline structures.

Comparison of the XRD patterns of the crystalline phases of FA and the mix of FA-CH-sand-water at 7 days and 28 days is shown in Fig. 11. In this case, the presence of mullite ( $\text{Al}_6\text{Si}_2\text{O}_{13}$ ), quartz ( $\text{SiO}_2$ ), calcite ( $\text{CaCO}_3$ ), and albite ( $\text{AlSi}_3\text{O}_8$ ) was identified. Comparison of the XRD patterns of the crystalline phases of BD and the mix of BD-CH-sand-water at 7 days and 28 days is shown in Fig. 12. In the case of BD, the presence of quartz ( $\text{SiO}_2$ ), calcite ( $\text{CaCO}_3$ ), and albite ( $\text{AlSi}_3\text{O}_8$ ) was also identified, in addition to gypsum ( $\text{Ca}(\text{SO}_4(\text{H}_2\text{O})_2)$ ), anorthite ( $(\text{CaNa})(\text{AlSi})_2\text{Si}_2\text{O}_8$ ), and other silico-aluminum crystals. Again, the calcite presence increased with time. In all cases, for BSA and more evident for FA and BD, there was an increment in crystallinity phase with time.

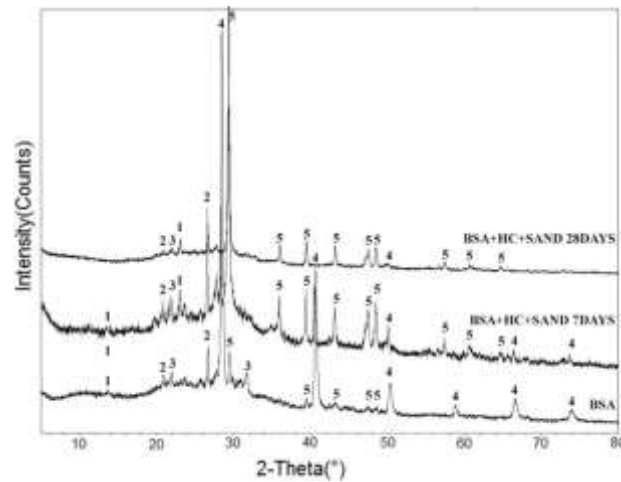


**Fig. 10.** Evolution of crystalline phases during the pozzolanic reaction by XRD of BSA: (1) anorthoclase ( $\text{AlSi}_3\text{O}_8$ ), (2) quartz ( $\text{SiO}_2$ ), (3) albite ( $\text{AlSi}_3\text{O}_8$ ), (4) sylvite ( $\text{KCl}$ ), and (5) calcite ( $\text{CaCO}_3$ )

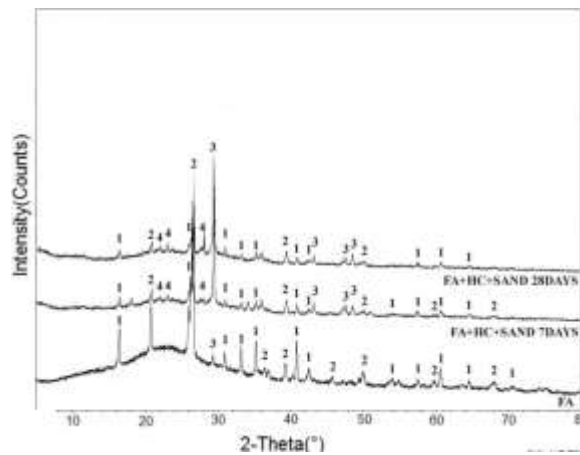


**Fig. 11.** Evolution of crystalline phases during the pozzolanic reaction by XRD of FA: (1) mullite ( $\text{Al}_6\text{Si}_2\text{O}_{13}$ ), (2) quartz ( $\text{SiO}_2$ ), (3) calcite ( $\text{CaCO}_3$ ), and (4) albite ( $\text{AlSi}_3\text{O}_8$ )

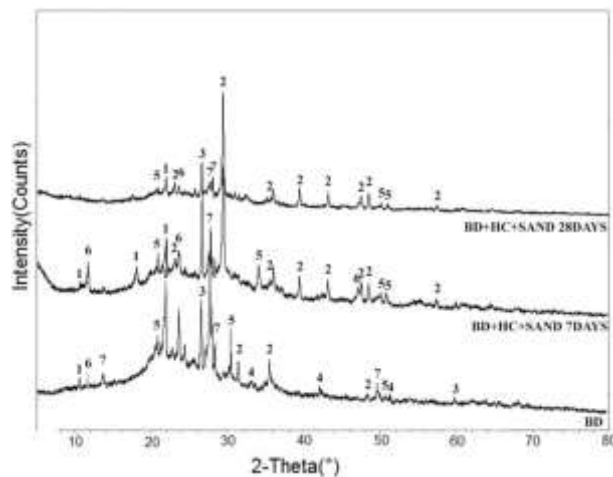


**Fig. 12.** Evolution of crystalline phases during the pozzolanic reaction by XRD of BD: (1) cordierite ( $\text{Mg}_2(\text{Al}_4\text{Si}_5\text{O}_{18})$ ), (2) calcite ( $\text{CaCO}_3$ ), (3) quartz ( $\text{SiO}_2$ ), (4) gypsum ( $\text{Ca}(\text{SO}_4(\text{H}_2\text{O})_2)$ ), (5) brushite ( $\text{CaPO}_3(\text{OH})_2(\text{H}_2\text{O})$ ), (6) meixnerite ( $(\text{Mg}_5\text{Al}_3(\text{OH})_{16})(\text{OH})_3(\text{H}_2\text{O})_4$ ), and (7) anorthite ( $(\text{CaNa})(\text{AlSi})_2\text{Si}_2\text{O}_8$ )

The evolution of morphology and microstructure during the pozzolanic reaction was examined using a scanning electron microscope (SEM) micrograph of the same specimens used in the evolution of crystalline phases analysis and lime-pozzolana compressive strength development test. Figures 13 and 14 show how new microstructures were created with the reaction between BSA, CH, and sand after 28 days.

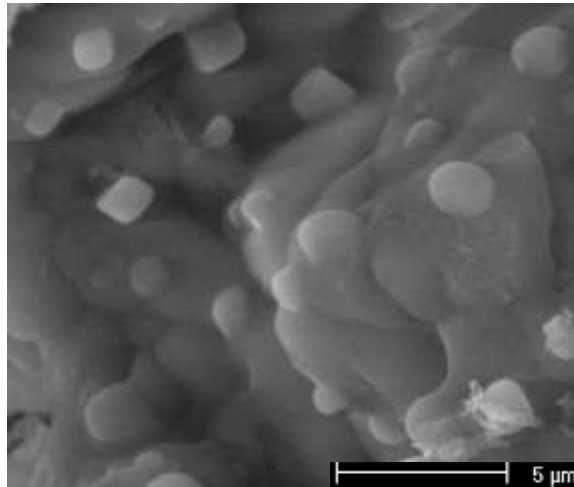


**Fig. 13.** SEM micrograph of BSA, zoom 5000x

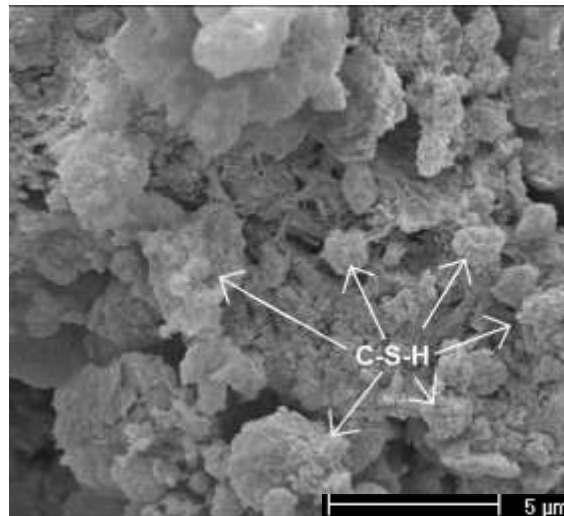


**Fig. 14.** SEM micrograph of BSA+CH+Sand after 28 days, zoom 5000x

New crystalline microstructures were observed wrapping the original quasi-spheres present in the BSA SEM micrograph. New microstructures were observed comparing the SEM micrograph of BD and FA with BD-CH-sand and FA-CH-sand after 28 days (Figs. 15, 16, 17, and 18).

Figure 17 shows fly ash characteristic xenospheres, and Figure 18 clearly shows new crystalline microstructures around these xenospheres, joining the different elements and creating new microstructures.

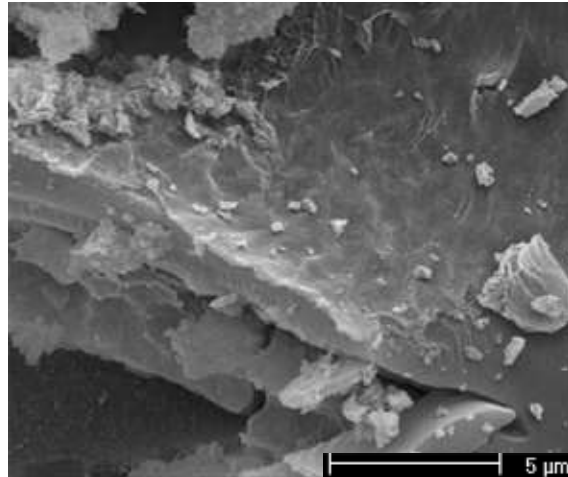


**Fig. 15.** SEM micrograph of BD, zoom 5000x

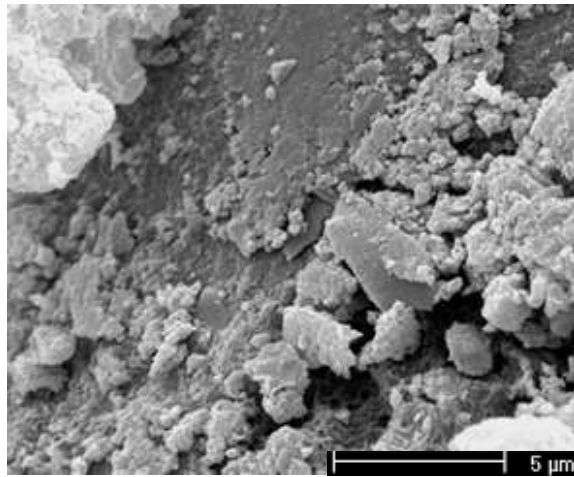


**Fig. 16.** SEM micrograph of BD+CH+Sand after 28 days, zoom 5000x

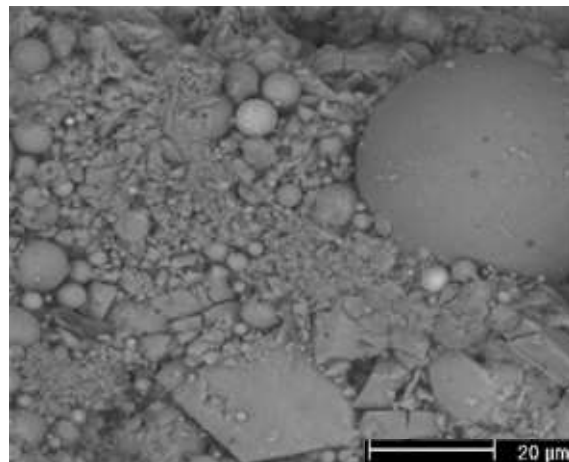


**Fig. 17.** SEM micrograph of FA, zoom 1000x

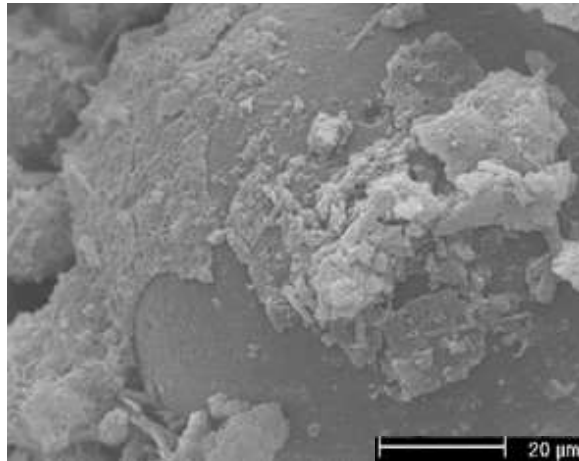


**Fig. 18.** SEM micrograph of FA+CH+sand after 28 days, zoom 1000x

These SEM micrographs show how pozzolanas can be activated by CH in combination with sand and water after 28 days at controlled conditions and how new microstructures can be created. A connection between the evolution of crystalline phases was observed during the pozzolanic reaction by XRD of BSA, FA, and BD and the specimens of BSA-CH-sand-water, FA-CH-sand-water, and BD-CH-sand-water and the new microstructures detected in the SEM micrograph.

It would be useful and necessary to study controlled calcined BSA with controlled temperature and times to compare the results to determine the importance of temperature and time of calcination.

## CONCLUSIONS

1. The chemical composition of barley straw ash (BSA) as determined by XRF showed a medium concentration of reactive silica and aluminum. Both recycled dust of fired clay brick (BD) and fly ash (FA) showed higher concentrations of reactive silica and aluminum and a good concentration of iron. This indicates a better chance for BD and FA to react with calcium hydroxide (CH) and more of a chance to constitute a cementitious material.
2. By XRD, BSA presented a 50% amorphous phase, but BD presented a better proportion of percentage of amorphous phase from a graphical and qualitative comparison. From XRD, the crystalline phases could be identified as aluminosilicates, something characteristic of other pozzolans with good pozzolanic characteristics.
3. By XRD the presence of potassium chloride (KCl) was detected in BSA and wheat straw ash (WSA). A High content of KCl can be harmful for the pozzolanicity of the material. As was forementioned, there is reference about how BSA could be used as a pozzolanic material in previous studies, and BSA and WSA present similar XRD results and pozzolanicity results. It is concluded that the pozzolanic behavior depends on the other compounds and microstructure detected in BSA and WSA, even in the presence of KCl. This is reaffirmed with the typical microstructures of C-S-H shown by SEM, which is a sign of good pozzolanic behavior. However, the high content of

KCl could be responsible for the lower pozzolanicity of BSA and WSA in comparison with BD and FA.

4. From SEM analysis, it was possible to determine a change between the microstructure, but it was not clear enough to determine which had better or worse response in that time.
5. Based on the results obtained, both BD and FA were shown to improve the compressive strength development test comparison. This may be ascribed to a higher pozzolanic activity, at the early ages of the pozzolanic reaction, which leads to the formation of calcium hydroxide solution (CHS) products due to the reaction between the pozzolan and calcium hydroxide present in the system.
6. In addition, the pozzolanic reactivity may depend on the complexity of its composition and crystallography. Different compounds have different response in contact with saturated  $\text{Ca}(\text{OH})_2$  in the solution time, influencing in the speed and on the duration of the reaction. In this work and since the pozzolanic material had the same particle size and fineness, greater pozzolanic reactivity was observed in BA and FA, compared to the other materials.
7. The electrical conductivity measurements method (ECMM) is a reliable technique for observing the pozzolanic activity of the materials and allows a qualitative evaluation of the pozzolanic reactivity between different materials.
8. It is concluded that BSA is a pozzolanic material with a good reactivity. However, it exhibits less pozzolanic activity in comparison with BA and FA.

## ACKNOWLEDGMENTS

The authors are grateful for the support of CONACYT, Universidad Autónoma de Querétaro, and especially grateful for the support of Adair Jimenez and Eleazar Urbina from the laboratory LITRA of CINVESTAV. The authors are grateful to Carmen Peza Ledesma from the laboratory of Electronic Microscopy of CFATA-UNAM and Beatriz Millán Malo from the laboratory of X-ray diffraction of CFATA-UNAM. The authors are also grateful for the logistics support to “Parque Nacional Iztaccíhuatl – Popocatepetl” and to the “INIFAP-Campo Experimental Bajío.”

## REFERENCES CITED

- Al-Akhras, N. M., and Abu-Alfoul, B. A. (2002). “Effect of wheat straw ash on mechanical properties of autoclaved mortar,” *Cem. Concr. Res.* 32(6), 859-863. DOI: 10.1016/S0008-8846(02)00716-0
- Amigó, V., Guzmán, A., Gutiérrez, C., Delvasto, S., and Mejía de Gutiérrez, R. (2011). “Valoración puzolánica de la hoja de la caña de azúcar,” *Mater. Construcc.* 61(302), 213-225. DOI: 10.3989/mc.2011.54809
- ASTM C 109 / C109M (2013). “Test for compressive strength of hydraulic cement mortars,” ASTM International, West Conshohocken, PA.
- ASTM C-125-13b (2013). “Standard terminology relating to concrete and concrete

- aggregates,” ASTM International, West Conshohocken, PA.
- ASTM C 305 (2013). “Practice for mechanical mixing of hydraulic cement pastes and mortars of plastic consistency,” ASTM International, West Conshohocken, PA.
- ASTM C 593-95 (2000). “Standard specification for fly ash and other pozzolans for use with lime,” ASTM International, West Conshohocken, PA.
- Bensted, J., and Munn, J. (2000). “A discussion of the paper “Study of pozzolanic properties of wheat straw ash by H. Biricik, F. AkoÉz, I. Berktaý and A.N. Tulgar,” *Cem. Concr. Res.* 30(9), 1507-1508. DOI: 10.1016/S0008-8846(00)00366-5
- Biricik, H., Akoz, F., Berktaý, I., and Tulgar, A., (1999). “Study of pozzolanic proprieties of wheat straw ash,” *Cem. Concr. Res.* 29(5), 637-643. DOI: 10.1016/S0008-8846(98)00249-X
- Cristelo, N., Glendinning, S., Miranda, T., Oliveira, D., Silva, R. (2012). “Soil stabilization using alkaline activation of fly ash for self-compacting rammed earth construction,” *Const. Build. Mater.* 36(), 727-735. DOI: 10.1016/j.conbuildmat.2012.06.037
- Edwards, B. (2008). *Guía Básica de la Sostenibilidad*, 2<sup>nd</sup> Ed., Gustavo Gili, Barcelona, Spain.
- Frías, M., Villar-Cociña, E., Sánchez de Rojas, M. I., and Valencia, E. (2005). “The effect that different pozzolanic activity methods has on the kinetic constants of the pozzolanic reaction in sugar cane straw-clay ash/lime systems: Application of a kinetic–diffusive model,” *Cem. Concr. Res.* 35(11), 2137-2142. DOI: 10.1016/j.cemconres.2005.07.005
- Frías, M., Villar-Cociña, E., and Valencia-Morales, E., (2007). “Characterisation of sugar cane Straw waste as pozzolanic material for Construction: Calcining temperatura and kinetic parameters,” *Waste Manag.* 27(4), 533-538. DOI: 10.1016/j.wasman.2006.02.017
- Gartner, E. M., and Macphee, D. E. (2011) “A physico-chemical basis for novel cementitious binders,” *Cem. Concr. Res.* 41(7), 736-749. DOI: 10.1016/j.cemconres.2011.03.006
- Karade, S. R. (2010). “Cement-bonded composites from lignocellulosic wastes,” *Constr. Build. Mater.* 24(8), 1323-1330. DOI: 10.1016/j.conbuildmat.2010.02.003
- Khangaonkar, P. R., Rahmat, A., and Jolly, K. G. (1992). “Kinetic study of the hydrothermal reacton between lime and rice-hush-ash silica,” *Cem. Concr. Res.* 22(4), 577-588. DOI: 10.1016/0008-8846(92)90008-J
- Lanas, J., and Pérez Bernal, J. L. (2004). “Mechanical properties of natural hydraulic lime-based mortars,” *Cem. Concr. Res.* 34(12), 2191-2201. DOI: 10.1016/j.cemconres.2004.02.005
- Lima, S. A., Varum, H., Sales A. and Neto, V. F. (2012). “Analysis of the mechanical properties of compressed earth block masonry using the sugarcane bagasse ash,” *Const. Build. Mater.* 35, 829-837. DOI: 10.1016/j.conbuildmat.2012.04.127
- Lima Souza, P. S., and Dal Molin, D. C. C. (2005). “Viability of using calcined clays, from industrial by-products, as pozzolans of high reactivity,” *Cem. Concr. Res.* 35(10), 1993-1998. DOI: 10.1016/j.cemconres.2005.04.012
- Larbi, J. A., and Bijen, M. J. M. (1990). “The chemistry of the pore fluid of silica fume blended cement systems,” *Cem. Concr. Res.* 20(4), 506-516. DOI: 10.1016/0008-8846(90)90095-F



- Madurwar, M. V., Ralegaonkar, R. V., and Mandavgane, S. A. (2013). "Application of agro-waste for sustainable construction materials: A review," *Const. Build. Mater.* 38, 872-878. DOI: 10.1016/j.conbuildmat.2012.09.011
- Malhotra, S. K., and Dave, N. G. (1999). "Investigations into the effect of addition of fly ash and burn clay puzzolana on certain engineering properties of cement composites," *Cem. Concr. Comp.* 21(4), 285-291. DOI: 10.1016/S0958-9465(99)00006-2
- Marín, M., Reyes, J. L., Manzano, A., Pineda, J., Hernández, M. A., Pérez, J. J., and Marroquín, A. (2011). "Effect of fly ash and hemihydrate gypsum on the properties of unfired compressed clay bricks," *Int. J. Phys. Sci.* 6(24), 5766-5773. DOI: 10.5897/IJPS11.935
- Mathur, V. K. (2005). "Composite materials from local resources," *Constr. Build. Mater.* 20(7), 470-477. DOI: 10.1016/j.conbuildmat.2005.01.031
- Martinez-Ramirez, S., Blancovarela, M., Erena, I., and Gener, M. (2006). "Pozzolanic reactivity of zeolitic rocks from two different Cuban deposits: Characterization of reaction products," *Appl. Clay. Sci.* 32(1-2), 40-52. DOI: 10.1016/j.clay.2005.12.001
- Mostafa, N. Y., El-Hemaly, A. S., Al-Wakeel, E. I., El-Korashy, S. A., and Brown, P. W. (2001). "Characterization and evaluation of the pozzolanic activity of Egyptian industrial by-products. I. Silica fume and dealuminated kaolin," *Cem. Concr. Res.* 31(3), 467-474. DOI: 10.1016/S0008-8846(00)00485-3
- Pacheco-Torgal, F., and Jalali, S. (2012). "Earth construction: Lessons from the past for future eco-efficient construction," *Constr. Build. Mater.* 29, 512-519. DOI: 10.1016/j.conbuildmat.2011.10.054
- Payá, J., Borrachero, M. V., Monzó, J., Peris-Mora, E. and Amahjour, F. (2001). "Enhanced conductivity measurement techniques for evaluation of fly ash pozzolanic activity," *Cem. Concr. Res.* 31(1), 41-49. DOI: 10.1016/S0008-8846(00)00434-8
- Poon, C. S., Lam, L., Kouw, S. C., Wong, Y. L., and Wong, R. (2001). "Rate of pozzolanic reaction of metakaolin in high-performance cement pastes," *Cem. Concr. Res.* 31(9), 1031-1306. DOI: 10.1016/S0008-8846(01)00581-6
- Ramasamy, V. and Biswas, S. (2008). "Mechanical properties and durability of rice husk ash concrete," *Int. J. Appl. Eng. Res.* 13(12), 1799-1811.
- Rosell-Lam, M., Villar-Cociña, E., and Frías, M. (2011). "Study on the pozzolanic properties of a natural Cuban zeolitic rock by conductometric method: Kinetic parameters," *Constr. Build. Mater.* 25(2), 644-650. DOI: 10.1016/j.conbuildmat.2010.07.027
- Rukzon, S. and Chindaprasirt, P. (2012). "Utilization of bagasse ash in high-strength concrete," *Mater. Design* 34, 45-50. DOI: 10.1016/j.matdes.2011.07.045
- Rukzon, S. and Chindaprasirt, P. (2014). "Use of rice husk-bark ash in producing self-compacting concrete," *Adv. Civil Eng.* (published online). DOI: 10.1155/2014/429727
- Sanchez de Rojas, M. I., Rivera, J., and Frías, M. (1999). "Influence of the microsilica state on pozzolanic reaction rate," *Cem. Concr. Res.* 29(6), 945-949. DOI: 10.1016/S0008-8846(99)00085-X
- Sinthaworn, S., and Nimityongskul, P. (2009). "Quick monitoring of pozzolanic reactivity of waste ashes," *Waste Manag.* 29(5), 1526-1531. DOI: 10.1016/j.wasman.2008.11.010
- Taylor, H. F. W. (1997). *Cement Chemistry*, Thomas Telford Services Ltd., London.
- Villar-Cociña, E., Valencia, E., González, R., and Hernández, J. (2003). "Kinetics of the pozzolanic reaction between lime and sugar cane straw ash by electrical conductivity

measurement: A kinetic-diffusive model,” *Cem. Concr. Res.* 33(4), 517-524. DOI: 10.1016/S0008-8846(02)00998-5

Villar-Cociña, E., Valencia-Morales, E., Santos, S., and Savastano, H. (2008). “Bamboo leaf ash as pozzolanic material: Study of the reaction kinetics and determination of the kinetic parameters,” *Tenth International Conference on Non-Conventional Materials and Technologies*, NOCMAT 2008, Cali, Colombia, 12-14 November, 2008.

Villar-Cociña, E., Morales, E. V., Santos, S. F., Savastano, H., and Frías, M. (2011). “Pozzolanic behavior of bamboo leaf ash: Characterization and determination of kinetics parameters,” *Cem. Concr. Comp.* 33(1), 68-79. DOI: 10.1016/j.cemconcomp.2010.09.003

Worrell, E., Price, L., Martin, N., Hendricks, C., and Meida, L. O. (2001). “Carbon dioxide emissions from the global cement industry,” *Ann. Rev. Energ. Environ.* 26, 303-329. DOI: 10.1146/annurev.energy.26.1.303

Article submitted: July 14, 2014; Peer review completed: February 5, 2015; Revised version received and accepted: March 17, 2015; Published: May 1, 2015.

DOI: 10.15376/biores.10.2.3757-3774